GEOPHYSICAL RESEARCH LETTERS, VOL. 25, NO.12, PAGES 2021-2024, JUNE 15, 1998

Spatial structure and gradients of ion beams observed by FAST

J. P. McFadden[1], C. W. Carlson[1], R. E. Ergun[1], F. S. Mozer[1], M. Temerin[1], W. Peria[1], D. M. Klumpar[2], E. G. Shelley[2], W. K. Peterson[2], E. Moebius[3], L. Kistler[3], R. Elphic[4], R. Strangeway[5], C. Cattell[6], and R. Pfaff[7]

Abstract. High time resolution measurements of ion distributions by the FAST satellite have revealed kilometer scale spatial structure in the low altitude auroral acceleration region. The low altitude edge of the acceleration region appears to contain fingers of potential that extend hundreds of kilometers along B but are only a few to tens of kilometers wide. These fingers of potential do not appear to be strongly correlated with the local current or total potential drop. Gradients in the ion beam energy are found to be consistent with the electric field signatures expected in the quasi-static potential drop model of auroral acceleration. Typical ion beams show gradients of 0.5-1.0 keV/km, with some events as large a 3 keV/km. Integrations of the electric field along the spacecraft velocity are used to calculate parallel potential below FAST and are found to agree well with the ion beam energy for most events. One event is shown where an apparent temporal change in the auroral configuration occurs at the edge of the ion beam producing a disagreement between the beam energy and inferred potential.

Introduction

The observations of upgoing ion beams [*Shelley et al.*, 1976], of the associated density cavities [*Persoon et al.*, 1988], of a decrease in precipitating electron energy and a simultaneous increase in the electron loss cone and upgoing ion energy [*Mizera and Fennell*, 1977; *Croley, et al.*, 1978], and of electrostatic shocks correlated with ion beams [*Mozer et al.*, 1980; *Redsun et al.*, 1985] have provided strong evidence for the quasi-static potential drop model of auroral acceleration. This model postulates the formation of broad regions with U-shaped or ⌙-shaped potential contours that contain electric fields parallel to the magnetic field. Dual satellite comparisons of plasma data [*Reiff et al.*, 1988; *Burch*, 1988] have also supported this model. Integration of the electric field along the spacecraft path to infer the potential drop below the spacecraft for comparison with the ion beam energy is the most direct method of testing the potential drop model [*Temerin et al.*, 1981; *Redsun et al.*, 1985; *Marklund*, 1993]. Although these comparisons have been somewhat successful, they require that the auroral configuration be static for at least a couple of spacecraft spins. The time resolution of the particle measurements has typically been the spacecraft spin period (3-20 seconds) which is often much longer than the time variations observed in the electric fields. However, the overall picture generated by these observations indicates that the potential drop model is consistent with the data on large scales (>20 km). In order to test the potential drop model on the smaller scale sizes observed in the dc electric fields, particle measurements must be able to resolve changes in the particle distribution function over a kilometer.

Recent FAST observations have shown that the ion beams exhibit structure on very short spatial scales near the lower altitude boundary of the acceleration region. FAST plasma analyzers measure the ion (3 eV - 25 keV) and electron (4 eV - 30 keV) distribution with 78 ms resolution [*Carlson and McFadden*, 1998]. The spacecraft is oriented relative to the magnetic field such that plasma analyzers measure full pitch angle distributions continuously. Analyzers include deflectors at their entrance aperture that steer their field-of-view to always include both the parallel and anti-parallel magnetic field line so the pitch angle distributions are complete. This is important since the auroral regions contain narrow beams of both ions and electrons which require complete angular coverage for the fitting and moment calculations used below. FAST also measures the full vector DC and AC electric field and magnetic field.

In order to test the potential drop model of auroral acceleration at small scales, we have compared auroral ion beam energies with electric field data. Below we present data from a single auroral crossing which contains ion beams that have characteristics similar to the 25 beam events analyzed. We eliminated events where the electric field sensor saturated during the ion beam, and have selected relatively short beam events (<15 seconds) to reduce the chance that time variations in the auroral configuration affect the results. The plasma sensors have a time resolution nearly 40 times higher than that of previous experiments, which allows spatial resolution of < 1 km. This provides the spatial resolution needed to resolve changes in the plasma within the large electric field structures or electrostatic shocks. We examine changes in the ion beam and precipitating electrons for comparison with the inferred potentials determined from the electric field experiment. These observations of upgoing ion beams and converging electrostatic shocks in the upgoing field aligned current region are similar to the results presented by *Carlson et al.* [1998] of upgoing electron beams and diverging electrostatic shocks in the downgoing current region.

Spatial Structure of Ion Beams

Figure 1 shows a 30 second stretch of data inside a pre-midnight auroral arc. The panels 1 and 2 are electron energy and pitch angle spectrograms which exhibit a typical inverted-V arc signature. Pitch angle spectrograms are displayed as -90° to 270° to reflect the analyzer's 360° field-of-view and to prevent narrow field aligned beams from appearing on the plot axes. Downward fluxes are at 0°. Panels 3 and 4 show the corresponding plots for the ions. The ion's angular distribution in panel 4 changes from a conic (peaked at ~135° and ~225°) to a beam (peaked at 180°) and

[1]Space Sciences Laboratory, University of California, Berkeley
[2]Lockheed Martin Palo Alto Research Laboratory, Palo Alto, CA
[3]University of New Hampshire, Durham
[4]Los Alamos National Laboratory, Los Alamos, NM
[5]University of California, Los Angeles
[6]University of Minnesota, Minneapolis
[7]Goddard Space Flight Center, Greenbelt, MD

Paper number 98GL00648.
0094-8534/98/98GL-00648$05.00

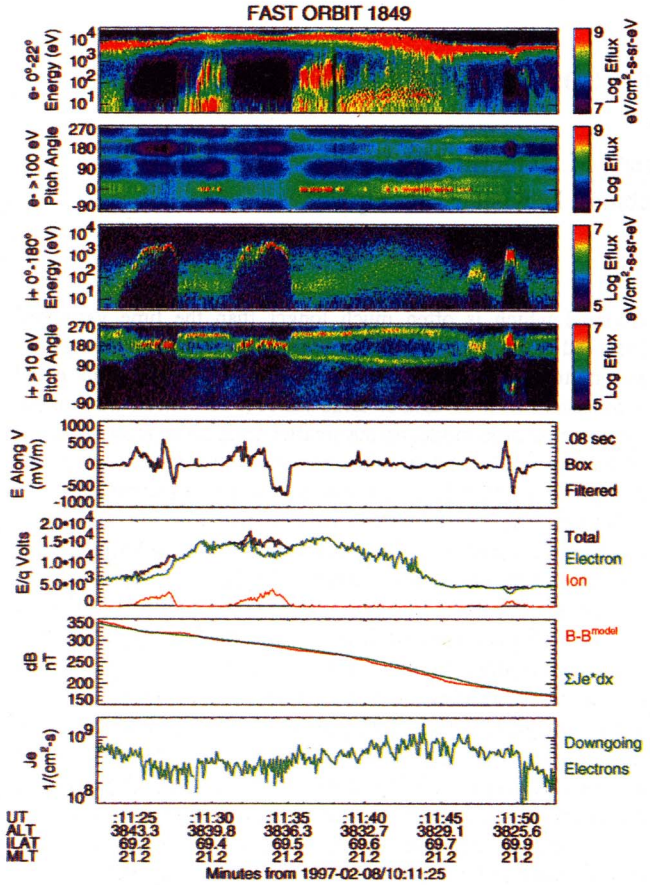

Figure 1. FAST burst data during 30 seconds of an inverted-V arc crossing show the ions (panels 3,4) transition back and forth from conics to beams. These transitions are accompanied by converging electrostatic shocks (panel 5), but are not correlated with any feature of the field aligned potential drop (panel 6) or current (panels 7,8).

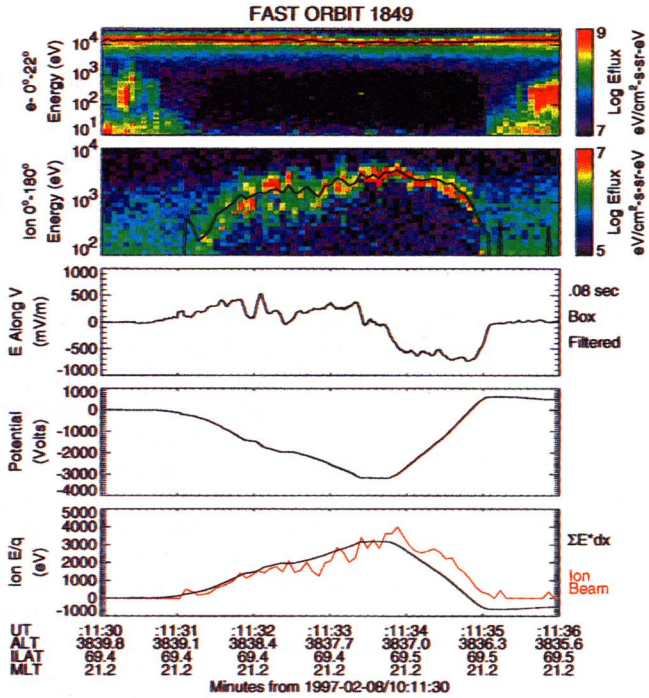

Figure 2. The characteristic energy of the ion beam (black line in panel 2, red line in panel 5) is compared to the implied parallel potential below the spacecraft (black lines in panels 4,5) determined by integrating the electric field along the spacecraft velocity (panel 3).

back to a conic several times across the arc. This feature of the lower edge of the acceleration region, with multiple beam/conic transitions, is common on those auroral crossing where beams are present. These transitions can be rather short, with some beams lasting for less than 1 second, corresponding to about 5 km perpendicular to **B** at 4000 km altitudes. The electron peak energy can be seen to drop and the loss cone to widen across these ion beams. What is unique about these data is that the ion beams are seen to correlate with even the shortest time scale features of the electric field. Panel 5 shows the electric field component perpendicular to **B** that lies nearly along the spacecraft velocity vector, V_{sc}. The electric field sensor has 32 kHz sampling, and the observations are smoothed here using a 0.08 second box filter to remove the large amplitude ion cyclotron waves and allow the DC fields to stand out. Large converging perpendicular electric fields, or electrostatic shocks, are correlated with all the ion beams even at these small spatial scales.

This structure in the ion distributions and fields demonstrates that the bottom of the acceleration region possesses a strong altitude dependance across the flux tubes. The parallel component of the electric field in the electrostatic shocks is normally small, $E_{\parallel} < 0.1E_{\perp}$. Exact determination of the parallel field in these structures is still in progress, requiring careful consideration of spacecraft attitude, the out of spin plane field component, spacecraft shadow and wake, density, and photoelectrons. However,

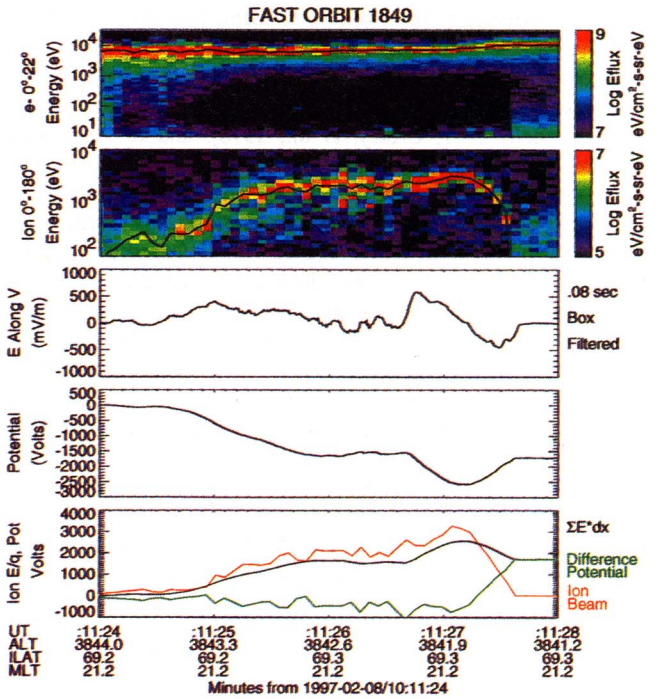

Figure 3. Same format as figure 2. In this case the ion energy and implied potential (panel 5) agree quite well until 10:11:27.2, where a 1500 V difference develops between the two (green). An ionospheric field would be > 1 V/m to account for the difference, suggesting that a temporal change in the auroral configuration has occurred instead. Small fluctuations and slowly varying trends in panel 5 are not significant and can be attributed to ion time of flight and ionospheric electric fields.

assuming the potential drop model and the upper limit on the parallel component allows us to estimate that these structures extend below the spacecraft at least 10 times their width. The 5-50 km wide beams should extend about 50-500 km below the spacecraft. Thus the lower edge of the acceleration region appears to contain long fingers of potential that extend along the magnetic field over at least 100 km scales.

The location of the ion beams does not appear to correlate with any local changes in the inferred potential drop. Panel 6 of figure 1 shows the characteristic energy of the ions (red) and electrons (green), along with the combined energy (black) which should represent the total of the potential above and below the spacecraft. The characteristic energies are determined by taking the ratio of the energy flux to particle flux of the beams. Of the four ion beam events, the first beam occurs at a gradient in the total potential drop, however the following three beams occur in regions where the total potential drop is the same on both sides of the beam. The last two ion beams also occur in a part of the arc where the total potential drop is about one third of the most energetic part of the arc, indicating there is no strong relationship between the lower boundary of the acceleration region and total potential drop.

Panel 7 shows the spin axis (eastward, perpendicular to $\mathbf{B_0}$ and $\mathbf{V_{sc}}$) component of the magnetic field minus a model field (red), along with the calculated magnetic deflection assuming a sheet current and using the integrated electron flux (green). The curves agree remarkably well and show that the entire current is carried by the energetic electrons. (No adjustment of instrument calibration was made to scale these plots, and only the initial dBz values were matched.) Panel 8 shows the electron flux, used in panel 7, varying slowly across the arc. These panels indicate that the total electron particle flux, or current, does not change in any significant way across the ion beams demonstrating that the lower altitude boundary of the acceleration region does not depend upon the local current. Without any correlation with the local precipitation signature, it seems likely that the altitude of the lower boundary is caused by the long-term evolution of the flux tube, including atmospheric scale height which has seasonal and solar cycle dependence.

The auroral acceleration region is known to be associated with a density cavity in the plasma. The evolution of an auroral arc is believed to proceed with a gradual erosion of the plasma along the flux tube as ions are accelerated away. The time history of the erosion should depend upon the initial plasma density profile on a flux tube, and on any replenishment mechanisms that provide additional plasma flow from the ionosphere to higher altitudes. An attempt was made to look at the upward ion flux across the ion beam/conic region and thus associate the beam location with a signature in the ion upwelling. A simple integral of the ion flux from the ion spectrometer proved inaccurate due to the large convection electric fields (panel 5) present in the ion beams. These large fields have an associated $\mathbf{E \times B}$ drift that can shift the ion beam direction by 5°-10° from $\mathbf{B}$, which is the order of the beam width and spectrometer field-of-view. This deflection can cause a factor of 2 to 3 under estimation of the ion flux within the ion beam. The estimated ion beam flux was ~30% of the adjacent upward flux of ion conics. However, we are unable to determine if this lower flux in the beam is due to $\mathbf{E \times B}$ associated errors in the calculation.

As a final word on the spatial structure of the ion beam events, we briefly point to the last beam in figure 1. This event is the only known observation of counterstreaming ions within hundreds of ion beam observations by FAST. The upgoing and downgoing peak energy track each other for nearly a second (10 analyzer sweeps) over an order of magnitude in energy. It appears that a local downward parallel field above FAST has reflected at least part of the upgoing ion beam. The downward beam eventually disappears, leaving only the upward beam, indicating a complicated spatial/temporal structure along the flux tube. Since this event represents a rare and perhaps temporal change in the auroral configuration, its discussion is limited to this reference as an unusual, narrow, ion beam event.

Gradients in Ion Energy

Not only are the general size of the ion beams and associated potential structures of interest, but also the perpendicular gradient scale of the ion beams. How steep a gradient in ion energy can be observed? Are these gradients spatial or temporal? Are changes in the ion beam energy and measured electric fields consistent with the potential drop model? To answer these questions, we integrated the perpendicular electric field across the ion beams for comparison with ion energy. Figure 2 shows details of the second beam from Figure 1 including the electron and ion fluxes, the perpendicular electric field along $\mathbf{V_{sc}}$, the integrated potential, and a comparison of integrated potential (black) with the ion beam characteristic energy (red). The characteristic energy is also shown on the ion and electron spectrograms as the dark line. Although the beams are composed of various species (H^+, He^+, O^+) with different densities and energies [*Moebius et al.*, 1998], the characteristic energy should reflect the potential drop if energy is primarily exchanged between the ions. The integrated potential is seen to agree remarkably well with the ion beam energy. The ions appear to react to the 800 mV/m electric fields as expected for a narrow potential structure. On the northern edge of the beam, the ion energy shows a steep gradient with a characteristic energy change of about 0.7 keV/km. Similar gradients in the ion energy have been observed in other ion beams, with corresponding electric field signatures.

The sharpest changes in ion beam characteristic energy have been about 5 keV in 1/3 of a second, or about 3 keV/km assuming a purely spatial variation. These strong gradients would have correspondingly large electric fields (3 V/m) that would saturate the electric field sensor, assuming purely spatial gradients. Ion beam events with saturated electric field signatures have not been included in this study. However, some of these rapidly varying ion events have corresponding electric field signatures that are much smaller than the beam gradients imply, indicating temporal variations are present as discussed below. For the 25 narrow (4-80 km) ion beams carefully investigated at this time, 15 have >0.5 keV/km variations in ion beam energy with comparable electric field signatures (>500 mV/m).

The integrated electric fields, which give implied potentials, do not always agree exactly with the ion beam energy. Figure 3 shows the first ion beam from figure 1. The bottom panel shows the ion beam characteristic energy (red), the integrated potential (black), and the difference between the two (green). The integrated potential agrees quite well with the ion beam energy until about 10:11:27.2. Between 10:11:27.2 and 10:11:27.6, a 1500 V difference develops between the ion beam energy and inferred potential. This difference could represent the variation in the ionospheric potential, however the implied ionospheric electric fields would be >1 V/m, which is much larger than observed ionospheric electric fields.

It is more likely that the potential jump reflects a temporal change in the auroral configuration. A change of the auroral currents, or an equivalent Alfven wave pulse that occurred as the spacecraft approached the edge of the ion beam, could give rise to

a time varying electric field whose integral contributes to the implied potential but which physically has no contribution to the static potential configuration. The time varying electric field would have to be the order of ~0.8 V/m in the northward (positive) direction, such as to cancel out part of the southward field leaving only -0.5 V/m in the electrostatic shock at 10:11:27.4. No evidence of a magnetic signature was observed above the 1-2 nT noise level indicating $\Delta E/\Delta B>c$, however narrow spatial width Alfvenic structures may have $\Delta E/\Delta B>c$ [*R. Lysak*, private communication].

An alternative explanation of the temporal variation is that a reconfiguration of the quasi-static potential occurred along the field line. The out-of-spin-plane component of the electric field has a significant electric field that roughly tracks the spin plane component perpendicular to $\mathbf{B}_0$, making the local shock structure at an angle of about 50° relative to $\mathbf{V}_{sc}$. A southward motion of the electrostatic shock structure, with velocity slightly greater than the velocity of FAST (V_{sc}=5.6 km/s) would be required to account for the difference in integrated potential and ion beam energy. Since the lower boundaries of electrostatic shocks must be oblique to **B**, a southward motion is equivalent to an upward vertical motion of the potential structure. Motion of this lower boundary is not Alfvenic since it represents charge redistribution in a region with parallel electric fields where the MHD assumptions break down.

It has been speculated that the acceleration region may contain strong double layers (large parallel electric fields) which have eluded detection since they are assumed to be rather small in vertical extent. One might expect an upward motion of the acceleration region to be accompanied by a strong double layer. The deconvolution of the electric field contains a strong upward parallel electric field, ~300 mV/m (not shown), as FAST exits the ion beam. The perpendicular field is of the same magnitude, ~500 mV/m, and a preliminary investigation indicates the signature is real. However, because of the rarity of such measurements and the large number of instrumental effects that can give false signatures, we reserve final judgement on this observation until a later time. If further investigation confirms this parallel electric field, and similar examples can be found, these observations could support a theory that describes the interface at the bottom of the acceleration region.

Summary

High time resolution measurements of ion distributions in the low altitude auroral acceleration region have revealed kilometer scale spatial structure in the lower boundary. The low altitude edge of the acceleration region appears to contain fingers of potential that extend hundreds of kilometers along **B** but are only few to tens of kilometers wide. These fingers of potential do not appear to be strongly correlated with the local current or total potential drop. Without any correlation with the local precipitation signature, it seems likely that the altitude of the lower boundary is caused by the long-term evolution of the flux tube.

Gradients in the ion beam energy are consistent with the electric field signatures expected in the quasi-static potential drop model of auroral acceleration. Typical ion beams show gradients of 0.5-1.0 keV/km and have comparable 0.5-1.0 V/m electric field signatures. Gradients in ion energy as large as 3 keV/km have been observed. Integrations of the electric field along the direction of the spacecraft velocity are used to calculate the parallel potential below FAST and found to agree well with the ion beam energy for most events. This shows that the ionosphere is largely decoupled from the magnetosphere. One event is shown where an apparent temporal change in the auroral configuration occurs at the edge of the ion beam producing a disagreement between the beam energy and inferred potential. A vertical motion of the acceleration region, which is equivalent to a southward motion of the electric field structure, may account for the discrepancy. A large parallel electric field signature is currently being investigated as a possible strong double layer seen during this auroral reconfiguration.

Acknowledgments. The analysis of FAST data was supported by NASA grant NAG5-3596.

References

Burch, J. L., Simultaneous plasma observations with DE-1 and DE-2, Adv. Space Res., **8**, 353, 1988.

Carlson C. W., and J. P. McFadden, Design and applications of imaging plasma instruments, *AGU Monog. Meas. Techn. Space Plasmas*, ed. R. Pfaff, in press, 1998.

Carlson, C. W., et al., FAST observations in the downward auroral current region: Energetic upgoing electron beams, parallel potential drops, and ion heating, Geophys. Res. Lett., in press, 1998.

Croley, D. R., Jr., P. F. Mizera, and J. F. Fennell, Signature of a parallel electric field in ion and electron distributions in velocity space, J. Geophys. Res. **83**, 2701, 1978.

Marklund, G., Viking investigations of auroral electrodynamical processes, J. Geophys. Res. **98**, 1691, 1993.

Mizera, P. F., and J. F. Fennell, Signatures of electric fields from high and low altitude particle distributions, Geophys. Res. Lett., **4**, 311, 1977.

Moebius, E., et al., Species dependent energies in upward directed ion beams over auroral arcs as observed with FAST TEAMS, Geophys. Res. Lett., in press, 1998.

Mozer, F. S., C. A. Cattell, M. K. Hudson, R. L. Lysak, M. Temerin, and R. B. Torbert, Satellite measurements and theories of low altitude auroral particle acceleration, Space Sci. Rev., **27**, 155, 1980.

Persoon A. M., D. A. Gurnett, W. K. Peterson, J. H. Waite, Jr., J. L. Burch, and J. L. Green, Electron density depletions in the nightside auroral zone, J. Geophys. Res., **93**, 1871, 1988.

Redsun, M. S., M. Temerin, and F. S. Mozer, Classification of auroral electrostatic shocks by their ion and electron associations, J. Geophys. Res., **90**, 9615, 1985.

Reiff, P. H., H. L. Collin, J. D. Craven, J. L. Burch, J. D. Winningham, E. G. Shelley, L. A. Fran, and M. A. Friedman, Determination of auroral electrostatic potentials using high and low-altitude particle distributions, J. Geophys. Res., **93**, 7441, 1988.

Shelley, E. G., R. D. Sharp, and R. G. Johnson, Satellite observations of an ionospheric acceleration mechanism, Geophys. Res. Lett., **3**, 654, 1976.

Temerin, M., M. H. Boehm, and F. Mozer, Paired electrostatic shocks, Geophys. Res. Lett., **8**, 799, 1981.

C. Cattell, University of Minnesota, Minneapolis, MN 55455
R. Elphic, Los Alamos National Lab, Los Alamos, NM 97545
D.M. Klumpar, E. Shelley, and W. K. Peterson, Lockheed Martin Palo Alto Research Laboratory, Palo Alto, CA 94304
J. P. McFadden, C. Carlson, R. Ergun, F. Mozer, M. Temerin, and W. Peria, Space Sciences Laboratory, University of California, Berkeley, CA 94720-7450. (e-mail: mcfadden@ssl.berkeley.edu)
E. Moebius, L. Kistler, U. of New Hampshire, Durham, NH 93824
R. Pfaff, Goddard Space Flight Center, Greenbelt, MD 20771
R. Strangeway, University of California, Los Angeles, CA 90095

(Received November 10, 1997; revised January 13, 1998;
accepted January 14, 1998.)